Desalination 269 (2011) 157–162

Contents lists available at ScienceDirect

Desalination

journal homepage: www.elsevier.com/locate/desal

Modeling and optimization of voltage and treatment time for electrocoagulation removal of hexavalent chromium

Manpreet S. Bhatti [a], Akepati S. Reddy [b], Rajeev K. Kalia [c], Ashwani K. Thukral [a,*]

[a] Department of Botanical and Environmental Sciences, Guru Nanak Dev University, Amritsar-143005, Punjab, India
[b] Department of Biotechnology and Environmental Sciences, Thapar University, Patiala-147001, Punjab, India
[c] Control and Instrumentation Maintenance Circle, GGSS Thermal Power Plant, Rupnagar, Punjab, India

ARTICLE INFO

Article history:
Received 14 July 2010
Received in revised form 4 October 2010
Accepted 18 October 2010
Available online 13 November 2010

Keywords:
Cr(VI) removal
Statistical modeling
Response surface methodology
Artificial neural network
Desirability plot
Design-Expert software

ABSTRACT

The present study was undertaken to optimize process variables, electrolysis voltage and treatment time for the electrocoagulation removal of hexavalent chromium (Cr(VI)). Response surface methodology (RSM) with center composite design was used to achieve energy efficient removal of Cr(VI). Predictive models using ANOVA and multiple response optimization revealed that optimal Cr(VI) removal efficiency occurred at 11 V and 18.6 min treatment time to give 50 % Cr(VI) removal efficiency with a consumption of 15.46 KWh m^{-3} energy. Multiple response optimization through a desirability function saves 32.3% energy consumption. The models explained 97.5% variability for Cr(VI) reduction efficiency and 99% variability for energy consumption. Artificial neural network (ANN) model was generated to validate the RSM predictions. Validation experiments were performed at proposed optimal conditions proved RSM and ANN predictions.

1. Introduction

Hexavalent chromium (Cr(VI)) is one of the most toxic constituents occurring in effluents discharged from chemical industries such as leather tanning, electroplating, oil refinery, textile, paints, pigments, glass manufacturing etc. Electroplating industry generates a high concentration of Cr(VI) in its effluents (140 mg/l), and leather tanning and textile mill effluents contain 10–50 mg/l and 5–20 mg/l of Cr(VI), respectively [1]. The discharge of Cr(VI) is strictly regulated as per prescribed standards [2]. Although there are a number of technologies available for the removal of heavy metals viz. precipitation, ion-exchange, adsorption and membrane processes [3], the most frequently used treatment process being used in India is a two step batch process involving chemical reduction of Cr(VI) to Cr(III) through the addition of reducing agents like sodium meta bisulfite or sulfur dioxide at pH <3, followed by raising of pH to 8–9.9 with lime, to precipitate $Cr(OH)_3$.

Metal removal through electrocoagulation has specific advantages in terms of high metal removal efficiency, instant start-up, compact treatment facility, less sludge formation and ease of operation [4–6]. Electrocoagulation has been successfully employed for the removal of metals [7–22], hardness from drinking water [23], dye wastewater [24,25], textile wastewater [26–28], industrial paint wastewater [29], and organic wastewater [30,31]. The electrocoagulation removal of Cr (VI) takes place either through Cr(VI) reduction to Cr(III) near the cathode surface and/or adsorption on $Al(OH)_3$ floc [16]. While optimizing the process conditions for Cr(VI) removal, the authors previously reported 49.6% Cr(VI) removal efficiency at an expense of 28 KWh m^{-3} at a pH of 5, voltage of 12.8 V, and treatment time of 24 min [18].

The present study was aimed at reduction in energy consumption during the electrocoagulation removal of Cr(VI) by parameter optimization for electrolysis voltage and treatment time. The response surface methodology (RSM) approach using the center composite design (CCD) was used for the experimental design [16–18,25–31]. Responses were best fitted using the ANOVA strategy. Mathematical models were developed from the experimental results for chromium removal efficiency and energy consumption. Response surface plots were studied for optimizing Cr(VI) removal efficiency while minimizing energy consumption. Artificial neural network (ANN) modeling has been used by few researchers for Cr(VI) and dye removal [20,24]. Finally, RSM predictions were validated through the ANN approach.

2. Materials and methods

2.1. Simulated wastewater

The analytical grade reagents and chemicals used in the present study were procured from the Central Drug House and Spectrochem,

* Corresponding author. Tel.: +91 183 2257621 (residence), +91 183 2258802x3192 (office), +91 9417019459 (Mobile); fax: +91 183 2258819.
E-mail addresses: mbhatti73@gmail.com (M.S. Bhatti), siva19899@gmail.com (A.S. Reddy), rkalia66@yahoo.com (R.K. Kalia), akthukral@rediffmail.com (A.K. Thukral).

0011-9164/$ – see front matter © 2010 Elsevier B.V. All rights reserved.
doi:10.1016/j.desal.2010.10.055

India. A 100-mg l^{-1} Cr(VI) solution with a conductivity of 2 m mho cm^{-1} (pH 5) was prepared using $K_2Cr_2O_7$ and KCl.

2.2. Experimental setup and procedure

The reactor was fabricated using 6 mm of acrylic sheet having an area of 4×7 cm^2 and a height of 30 cm [18]. Electrodes were rested on a support, 3 cm above the base, and engraved with grooves for keeping a fixed distance of 15 mm between the electrodes. The solution was continuously stirred during the experiment at 100 rpm using a 21-mm magnetic bar. Aluminum (Al) electrodes with a 5-mm thickness and an effective area of 5×20 cm^2 were used as Al–Al pair for wastewater treatment. The Al electrode examined using scanning electron microscope (SEM) equipped with energy dispersive X-ray analysis (Quanta F-200 FEI, Netherlands) was found to have 91.45% aluminum with C (6.26%), Mg (1.01%), Si (0.8%), and O (0.47%) as impurities.

Regulated DC power supply (Aplab, India L-3210) working in the range of 0–32 V and 0–10 A was used. The voltage was adjusted in the range of 2.3–20.7 V using constant voltage mode. The average of amperage from the start to the end of experiment was used for the determination of energy consumption. The ripple and the noise of the instrument were less than 0.04%.

pH and conductivity (m mho cm^{-1}) were measured with a digital pH meter (Equiptronics, India, EQ-610) and a digital conductivity meter (Systronics, India, 304) respectively. Cr(VI) was determined colorimetrically (Standard Methods, Method No. 3500-Cr D) [32]. A complexometric reagent (1,5-diphenylcarbazide MW 242.28) was used for Cr(VI) estimation at 540 nm using double beam UV-visible spectrophotometer (Systronics, India, 2202). The voltage was set at 5 levels, 2.3, 5, 11.5, 18 and 20.7 V, and five treatment times were used: 9.5, 12, 18, 24, and 26.5 min.

A total volume of 560 ml of Cr(VI) solution was taken in the plexiglass reactor and Al electrodes were submerged up to a depth of 20 cm in the solution with a 15-mm clear spacing to give an effective surface area of 100 cm^2. The voltage was set at the desired level and DC power supply switched on for the preset time. Treated wastewater was filtered through Whatman No. 1 filter paper and subsequently analyzed for Cr(VI). Cr(VI) removal efficiency and energy consumption were determined using Eqs. (1) and (2), respectively.

$$\text{Cr(VI) reduction efficiency}(\%) = (C_i - C_f)\,/\,Ci \times 100 \quad (1)$$

$$\text{Energy consumption}(Wh) = \text{volts} \times \text{amperes} \times h \quad (2)$$

where C_i and C_f represent the initial and final concentrations of Cr(VI) (mg l^{-1}), respectively.

2.3. Experimental design and modeling

A total of 13 experiments were performed as per Rotatable CCD [33] (Table 1). The last 5 experimental runs (standard order 9–13) were the repeat experiments to check variance in the experimentation. Linear and interaction models were developed using a multiple regression analysis to study main effects and interactive mechanism. The β-regression coefficients were computed to study the relative importance for model terms. Path analysis was studied using interaction model for direct and indirect effects of voltage and treatment time on Cr(VI) removal efficiency. Model fitting and graphical analyses were carried out using the Design-Expert software (Stat-Ease Inc., Minneapolis). Model selection and model building are depicted in Fig. 1. Goodness of fit was studied using *lack of fit*, coefficient of determination (R^2) and coefficient of variation (CV %). Signal to noise (S/N) was estimated from adequacy precision ratio, with ratio>4 being considered satisfactory for the model.

Before moving to graphical analysis, diagnostic data checking was performed to check any highly influencing responses. The diagnostic study is primarliy based on the model residuals and indicates the outliers in the response data. Finally, a diagnostic table was generated in terms of residual, leverage, internally studentized residuals (limit ±3 sigma), externally studentized residuals (checking outliers for large values), DFFITS (limit ±2) and Cook's distance [34]. Response transformation was studied for the following three criteria: (i) maximum to minimum response ratio, if>10, suggests the transformation of the data to improve the model, (ii) normal probability plot for a specific shape, and (iii) model lack of fit if significant suggests higher noise than the signal. The Box–Cox plot suggests [35] the best transformation (lambda value) at which the natural logarithm of the sum of squares of the residuals is minimum.

The selected models were generated both in terms of coded factors (standardized equations) and actual factors (unstandardized equations). The regression constants in the coded equation are unitless coefficients and are used for process understanding [33]. Predictive models were developed for Cr(VI) removal efficiency and energy consumption using ANOVA.

From the models developed, optimal parameter values were determined by simultaneously solving equations for maximizing Cr (VI) removal efficiency and minimizing energy consumption [36]. The optimal parameter values were validated through electrocoagulation experiments. Response surface plots were developed from model equations. These response surface plots are helpful in locating the optimized conditions [37]. In numerical optimization, each parameter is set at a desired goal (maximize, minimize, target, within range, and none), along with upper and lower limits for each

Table 1
Center composite design along with experimental and predicted responses for Cr(VI) removal efficiency and energy consumption.

Std order	Coded levels		Actual levels		Cr(VI) reduction efficiency (%)			Energy consumption (Wh)		
	Voltage	Time	Volt V	Time min	Experimental	ANOVA Predicted	ANN Predicted	Experimental	ANOVA Predicted	ANN Predicted
1	−1	−1	5	12	31.9	31.64	31.95	0.95	0.90	1.01
2	1	−1	18	12	48.72	48.62	48.62	16.74	17.14	16.85
3	−1	1	5	24	40.24	39.62	40.30	1.90	1.58	1.51
4	1	1	18	24	50.93	50.46	50.86	37.50	36.96	37.40
5	−1.41	0	2.3	18	31.05	31.52	31.00	0.207	0.30	0.33
6	1.41	0	20.7	18	50.93	51.19	51.08	38.81	38.59	38.68
7	0	−1.41	11.5	9.5	40.24	40.34	40.38	4.28	4.16	4.11
8	0	1.41	11.5	26.5	46.66	47.28	46.79	12.44	13.17	12.71
9	0	0	11.5	18	51.36	50.39	50.22	8.45	9.28	9.01
10	0	0	11.5	18	49.29	50.39	50.22	9.49	9.28	9.01
11	0	0	11.5	18	49.65	50.39	50.22	9.66	9.28	9.01
12	0	0	11.5	18	51.36	50.39	50.22	9.66	9.28	9.01
13	0	0	11.5	18	50.29	50.39	50.22	9.14	9.28	9.01

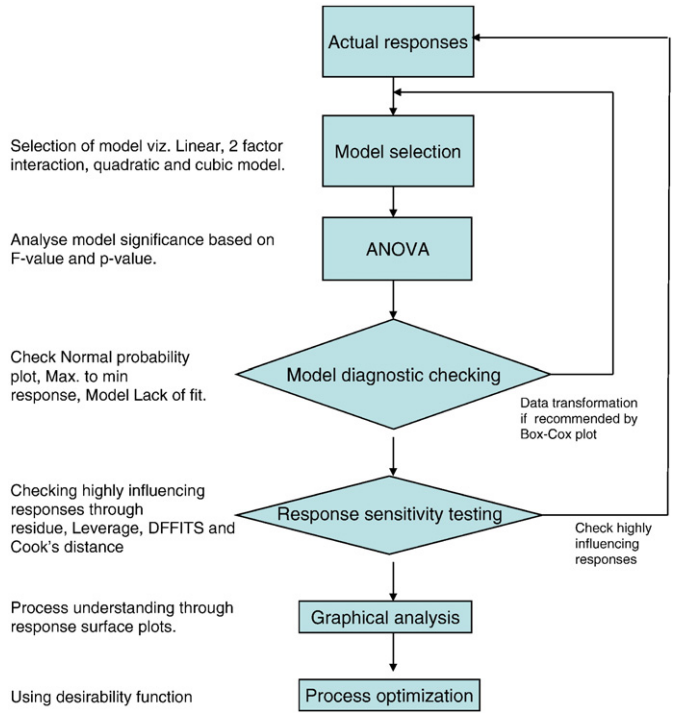

Fig. 1. Flow chart of model selection, model building and response optimization.

variable and equal relative importance. For numerical optimization, two responses were assigned equal weights and relative importance. Finally, the overall desirability function was generated, which ranges from 0 (least probability) to 1 (highest probability) of the goal achievement [36].

2.4. Artificial neural network modeling

ANNs are parallel computing systems, which can map almost any function of practical interest. Normalized CCD data (with range −1 to +1) were used to train the ANN model in MATLAB computing environment. Four neurons were chosen for the hidden layer. The sigmoidal transfer function was used for input to hidden layer mapping and a linear function for hidden layer to output layer mapping. The Bayesian regulation based function '*TRAINBR*' was used in the error backpropagation framework to train the network in MATLAB. Finally, the ANN model was used to validate the RSM predictions.

3. Results and discussion

3.1. Optimization for Cr(VI) removal efficiency and energy consumption

Cr(VI) removal efficiencies (response 1) obtained for the 13 experiments conducted are given in Table 1. From the main effects

Table 2
First order and interaction models for Cr(VI) removal efficiency.

Models for Cr(VI) removal efficiency		R^2	β-regression coefficients		
			Voltage	Time	Volt × Time
Main effects	25.92360 + 1.06970 × V + 0.40894 × min	0.6765	0.776	0.274	
Main effects with interaction	17.78956 + 1.77701 × V + 0.86083 × min − 0.039295 V × min	0.6911	1.288	0.576	−0.608
Two factor interaction	35.318 − 0.004960 V × time	0.588			0.767

Table 3
Path analysis of direct and indirect effect of voltage and treatment time on Cr(VI) removal efficiency.

Independent variables	Total effects R_{yx}	Direct effect	Indirect effect through interaction
X1: voltage	0.7756	1.288	−0.5132
X2: treatment time	0.2737	0.576	−0.3028

model (Table 2), voltage was found to have higher contribution than treatment time as indicated through β-regression coefficients. The interaction model slightly improves R^2 to 0.6911, whereas only two factor interaction model gave $R^2 = 0.588$. Path analysis (Table 3) revealed that both voltage and treatment time have positive direct effects but negative indirect effects on Cr(VI) removal efficiency. Therefore a second order interaction model was also attempted. A quadratic model provides best fit based on maximizing R^2 and not significant *lack of fit* (Table 4), implying thereby that it can be navigated in the design space. The *goodness of fit* gave 1.86% CV (excellent up to 5%) and predicted R^2 of 0.976. A model precision (S/N ratio) of 34.17 indicated a satisfactory signal to noise ratio. The selected model was statistically diagnosed for influencing model responses. The model diagnostic study revealed that all the responses are within the acceptable limits (Table 5). The quadratic model in terms of unitless regression coefficients is given in Eq. (3).

$$\text{Cr(VI) reduction efficiency}(\%) = 50.39 + 6.95\ \text{voltage} + 2.45\ \text{time} - 1.53\ \text{voltage x time} - 4.52\ \text{voltage}^2 - 3.29\ \text{time}^2 \quad (3)$$

where voltage and time are in coded units.

The multiple regression equation for actual factors is given in Eq. (4).

$$\text{Cr(VI) reduction efficiency}(\%) = 21.142 + 4.236\ \text{V} + 4.149\ \text{min} - 0.393\ \text{V x min} - 0.107\ \text{V}^2 - 0.091\ \text{min}^2. \quad (4)$$

Interaction between voltage and treatment time have an antagonistic effects as depicted by negative model term in Eq. (3). Response

Table 4
ANOVA table and model statistics for Cr(VI) removal efficiency and energy consumption.

Source	Cr (VI) reduction efficiency (%)		Sqrt. (Energy consumption) (Wh)	
	Quadratic model		Quadratic model	
	F-value	Prob. >F	F-value	Prob.>F
Model	177.751	<0.0001*	734.766	<0.0001*
Volt	538.881	<0.0001*	3312.692	<0.0001*
Time	67.107	<0.0001*	261.016	<0.0001*
Volt × time	13.089	0.0085*	68.390	<0.0001*
$Volt^2$	197.860	<0.0001*	19.873	0.0029*
$Time^2$	104.794	<0.0001*	8.025	0.0253*
Lack of fit	0.502	0.7009 (NS)	1.833	0.2813 (NS)
Model statistics				
CV %	1.858		3.194	
R^2	0.992		0.998	
Adjusted R^2	0.987		0.997	
Predicted R^2	0.976		0.991	

*Significant at $p \leq 0.05$.
NS = Not significant at $p \leq 0.05$.

Table 5
Diagnostic case statistics of quadratic model for Cr(VI) removal efficiency.

Std. order	Actual	Predicted	Residual	Leverage	Internally studentized residual	Externally studentized residual	Influence on fitted values DFFITS	Cook's distance
1	31.90	31.64	0.255	0.625	0.492	0.464	0.599	0.067
2	48.72	48.61	0.104	0.625	0.201	0.187	0.241	0.011
3	40.24	39.61	0.623	0.625	1.201	1.248	1.611	0.401
4	50.93	50.45	0.472	0.625	0.910	0.897	1.158	0.230
5	31.05	31.52	−0.471	0.625	−0.907	−0.894	−1.154	0.229
6	50.93	51.18	−0.257	0.625	−0.495	−0.467	−0.602	0.068
7	40.24	40.34	−0.104	0.625	−0.200	−0.186	−0.240	0.011
8	46.66	47.28	−0.624	0.625	−1.202	−1.250	−1.613	0.402
9	51.36	50.39	0.970	0.200	1.280	1.354	0.677	0.068
10	49.29	50.39	−1.100	0.200	−1.452	−1.608	−0.804	0.088
11	49.65	50.39	−0.740	0.200	−0.977	−0.973	−0.486	0.040
12	51.360	50.390	0.970	0.200	1.280	1.354	0.677	0.068
13	50.290	50.390	−0.100	0.200	−0.132	−0.122	−0.061	0.001

surface plots between Cr(VI) removal efficiency with voltage and treatment time depicted maximum Cr(VI) removal efficiency at about a 16-V and 19-min treatment time (Fig. 2). Running the quadratic model for maximizing Cr(VI) removal gave the optimum voltage of 12.8-V and 19.2-min treatment time. The predicted Cr(VI) removal efficiency was 51.9%, consuming 12.79 Wh of energy. Validation experiments conducted under the optimal parameters gave 52% Cr (VI) removal efficiency, in agreement with the predicted removal.

Results obtained for energy consumption (response 2) are given in Table 1. The quadratic model, best fit to the response data, had significant *lack of fit* ($p \leq 0.05$) and is thus not acceptable to navigate in the design space. Since the ratio of maximum to minimum response was 187.5 (> 10), the Box –Cox plot recommended square root transformation of the response data (Fig. 3). The quadratic model was again suggested as the best fit, and the model was found to be highly significant at 99.99% ($p<0.0001$) with no significant *lack of fit* ($p=0.281$) (Table 4). The *goodness of fit* gave CV of 3.19% and predicted R^2 equal to 0.990. The model S/N ratio was adequate (adeq. precision = 84.72). Model diagnostic studies are given in Table 6. Finally, the equation in terms of unitless regression coefficients is given in Eq. (5).

$$\text{Square root of Energy consumption (Wh)} = 3.05 + 2.00\ \text{voltage} + 0.56\ \text{time} + 0.41\ \text{voltage x time} + 0.17\ \text{voltage}^2 - 0.11\text{time}^2 \quad (5)$$

where voltage and time are in coded units.

The multiple regression equation for actual factors is given in Eq. (6).

$$\text{Square root of energy consumption (Wh)} = 0.45659 + 0.029746\ \text{V} + 0.079441\ \text{min} + 0.010439\ \text{V x min} + 0.003939\ \text{V}^2 - 0.0029377\ \text{min}^2. \quad (6)$$

The voltage and treatment time have synergistic effect on the energy consumption. Also, voltage has higher contribution in energy consumption than the treatment time due to positive model terms for volatge and voltage^2 (Eq. (5)). The response surface plot for energy consumption with voltage and treatment time showed the maximum energy consumption at 18-V and 24-min treatment time (Fig. 4).

3.2. Multiple response optimization

Model equations were solved maximizing Cr(VI) removal while minimizing energy consumption as per the criteria given in Table 7. Predicted numerical optimization was obtained at 11-V and 18.6-min treatment time with 50% Cr(VI) removal efficiency, consuming 8.66 Wh (15.46 KWh m^{-3}) energy. Voltage was a limiting factor due to the passivization of cathode beyond 11 V, thereby increasing energy consumption leading to the rise in temperature of the Cr(VI) solution. Validation experiments conducted at 11 V and 18.6 min gave 49.8% Cr (VI) removal efficiency consuming 8.60 Wh (15.35 KWh m^{-3}) energy as depicted in the desirability plot (Fig. 5). Model predictions validated at these optimal process conditions, are in agreement with the predicted responses (Table 7). The study revealed that beyond 11 V

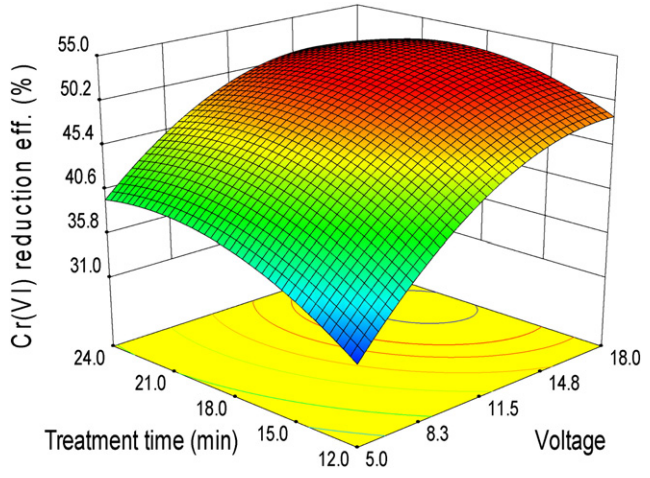

Fig. 2. Response surface plot showing the effect of voltage and treatment time on Cr(VI) removal efficiency.

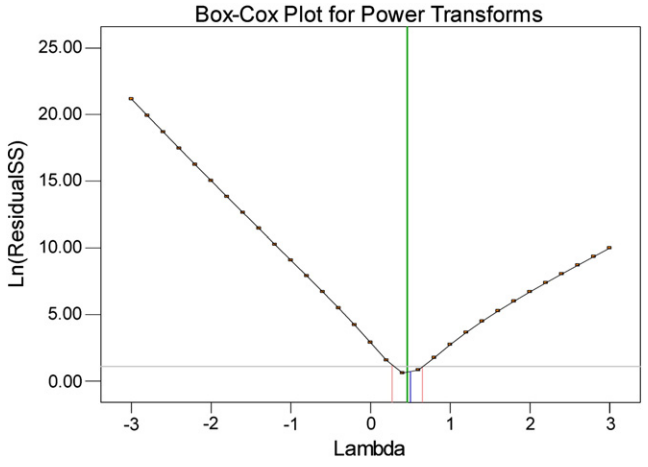

Fig. 3. Box–Cox plot showing optimized lambda for the transformation of energy consumption.

Table 6
Diagnostic case statistics of quadratic model for square root of energy consumption.

Std. order	Actual	Predicted	Residual	Leverage	Internally studentized residual	Externally studentized residual	Influence on fitted values DFFITS	Cook's distance
1	0.975	0.947	0.027	0.625	0.455	0.428	0.552	0.058
2	4.091	4.140	−0.049	0.625	−0.809	−0.787	−1.016	0.182
3	1.378	1.258	0.121	0.625	2.000	2.828	*3.65	*1.11
4	6.124	6.079	0.044	0.625	0.736	0.709	0.915	0.150
5	0.455	0.545	−0.090	0.625	−1.489	−1.668	*−2.15	0.616
6	6.230	6.212	0.018	0.625	0.299	0.278	0.359	0.025
7	2.069	2.039	0.030	0.625	0.497	0.469	0.605	0.069
8	3.528	3.629	−0.102	0.625	−1.688	−2.029	*−2.62	0.791
9	2.907	3.046	−0.138	0.200	−1.568	−1.802	−0.901	0.102
10	3.080	3.046	0.035	0.200	0.395	0.370	0.185	0.006
11	3.108	3.046	0.063	0.200	0.710	0.683	0.341	0.021
12	3.108	3.046	0.063	0.200	0.710	0.683	0.341	0.021
13	3.024	3.046	−0.022	0.200	−0.247	−0.230	−0.115	0.003

*Indicates exceeding the permissible diagnostic limits.

and 18.6 min treatment time, there is no appreciable increase in Cr(VI) reduction efficiency. One of the reasons could be the back conversion of Cr(III) to Cr(VI) in the solution due to oxidation at higher temperature. The left over Cr(VI) in the wastewater after the electrocoagulation, can be subjected to further electrocoagulation or some other treatment in series at downstream of the treatment facility.

3.3. ANN predictions

Using CCD experimental data, the ANN model was generated using voltage and treatment time as the input layer, four neurons in the hidden layer, and Cr(VI) removal efficiency and energy consumption as the output layer. The selected network architecture was trained for 60 iterations till the final trained network gave a mean square error of 0.0242. The weights and biases associated with the final trained network are given in Table 8. RSM optimized process conditions were validated using the ANN model. Voltage (11 V) and treatment time (18.6 min) were used as input parameters for the ANN model. An ANN predicted Cr(VI) removal efficiency of 49.61%, with 8.45 Wh (15.08 KWh m^{-3}) of energy consumption.

4. Conclusions

In the present study, a maximum of 51.9% Cr(VI) removal efficiency was achieved at a 12.8-V and 19.2-min treatment time, consuming 12.8 Wh (23 KWh m^{-3}) energy. Multiple response optimization for maximizing Cr(VI) removal efficiency and minimizing energy consumption gave a voltage of 11 V and 18.6-min treatment time as optimal points. Cr(VI) removal efficiency was 50% at these new optimal points consuming 8.66 Wh (15.46 KWh m^{-3}) energy. The study has shown that beyond a voltage of 11 V and 18.6-min treatment time, there is no appreciable increase in Cr(VI) removal efficiency. Low voltage with increased treatment time suggests better results in terms

Table 7
Criteria for multiple response optimization with RSM and ANN predictions.

Parameter	Goal	Upper limit	Lower limit	Lower weight	Upper weight	Importance
Voltage	Is in range	5	18	1	1	3
Treatment time	Is in range	12	24	1	1	3
Cr(VI) removal eff.	Maximize	31.05	51.36	1	1	3
Energy consumption	Minimize	0.207	38.81	1	1	3
Validation experiment		Voltage	Treatment time		Cr(VI) rem. eff. (%)	Energy (Wh)
Validation experiment at optimized process conditions		11 V	18.6 min		49.80	8.60
RSM predictions		11 V	18.6 min		50.0	8.66
ANN predictions		11 V	18.6 min		49.61	8.45

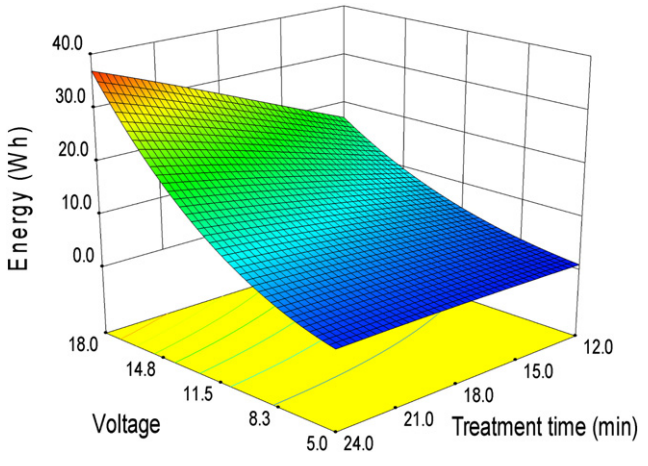

Fig. 4. Response surface plots showing the effect of voltage and treatment time on energy consumption.

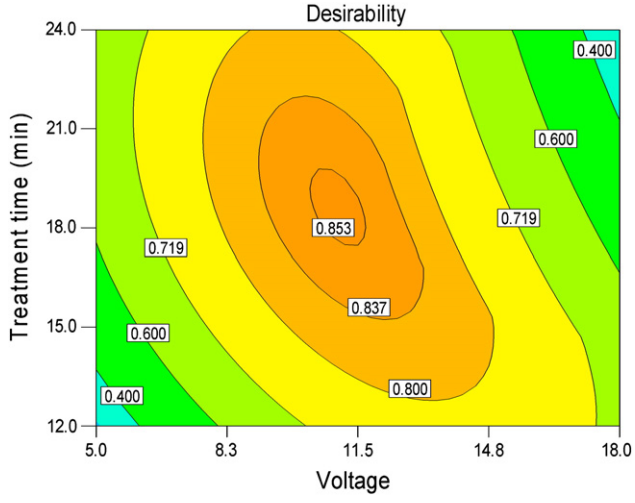

Fig. 5. Desirability plot showing goal optimization.

Table 8
Network weights and biases for ANN model.

	Weights between input layer and hidden layer			Weights between hidden layer and output layer	
	Input neuron 1	Input neuron 2	Bias	Output neuron 1	Output neuron 2
	Voltage	Treatment time		Cr(VI) removal eff.	Energy consumption
Hidden neuron 1	1.5527	0.5633	−1.1457	−0.4161	0.2129
Hidden neuron 2	1.1107	0.7920	0.5265	1.0843	−0.0774
Hidden neuron 3	0.0941	1.1411	0.6009	−0.4643	−2.1168
Hidden neuron 4	−1.2128	0.8422	−0.4350	−1.4642	−0.7392
				Bias −0.9909	Bias 0.1599

of maximizing Cr(VI) removal efficiency and minimizing energy consumption. The electrode potential significantly increases beyond 11 V, whereas a treatment time of 20 min is practically acceptable for the treatment process. Furthermore, multiple response optimization saves 32.3% energy by decreasing energy consumption from 23 KWh m^{-3} to 15.46 KWh m^{-3}, whereas Cr(VI) removal efficiency was marginally reduced. In our previous work, the optimized parameters (pH 5, 12.83 V, and 24 min) gave 49.6% Cr(VI) removal efficiency consuming 28 KWh m^{-3}. New process conditions (11 V and 18.6 min) reduce energy consumption by 44.8% while maintaining comparable Cr(VI) removal efficiency [18]. The predicted quadratic model showed a high coefficient of determination for Cr(VI) removal ($R^2 = 0.975$) and energy consumption ($R^2 = 0.990$). RSM predictions are also validated using the ANN approach.

Acknowledgements

The authors are thankful to the University Grants Commission, New Delhi, for financial support; Head, Department of Botanical and Environmental Sciences, Guru Nanak Dev University, Amritsar, for providing research facilities; and the Indian Institute of Technology, Roorkee, for the metal composition of the Al electrode using SEM-EDX.

References

[1] S.A. Abassi, N. Abassi, R. Soni, Heavy metals in the environment, Mittal Publications, New Delhi, 1997.
[2] Pollution Control Law Series, Pollution Control Acts, Rules and Notifications Issued Thereunder, CPCB, Ministry of Environment and Forests, Govt. of India, New Delhi, 2001.
[3] W.W. Eckenfelder Jr., Industrial Water Pollution Control, 3rd ed., McGraw Hill, Singapore, 2000.
[4] G. Chen, Electrochemical technologies in wastewater treatment, Sep. Purific. Technol. 38 (2004) 11–41.
[5] M.Y.A. Mollah, P. Morkovsky, J.A.G. Gomes, M. Kesmez, J. Parga, D.L. Cocke, Fundamentals, present and future perspective of electrocoagulation, J. Hazard. Mater. B114 (2004) 199–210.
[6] M.Y.A. Mollah, R. Schennach, J.R. Parga, D.L. Cocke, Electrocoagulation (EC)-science and application, J Hazard. Mater. B84 (2001) 29–41.
[7] J.A.G. Gomes, P. Daida, M. Kesmez, M. Weir, H. Moreno, J.R. Parga, G. Irwin, H. McWhinney, T. Grady, E. Peterson, D.L. Cocke, Arsenic removal by electrocoagulation using combined Al-Fe electrode system and characterization of products, J. Hazard. Mater. 139 (2007) 220–231.
[8] A. Shafaei, M. Rezayee, M. Arami, M. Nikazar, Removal of Mn2+ ions from synthetic wastewater by electrocoagulation process, Desalination 260 (2010) 23–28.
[9] G. Sayiner, F. Kandemirli, A. Dimoglo, Evaluation of boron removal by electrocoagulation using iron and aluminum electrodes, Desalination 230 (2008) 205–212.
[10] K. Thella, B. Verma, V.C. Srivastava, K.K. Srivastava, Electrocoagulation study for the removal of arsenic and chromium from aqueous solution, J. Env. Sci. Health. Part A 43 (2008) 554–562.
[11] D. Ghosh, H. Solanki, M.K. Purkait, Removal of Fe(II) from tap water by electrocoagulation technique, J. Hazard. Mater. 155 (2008) 135–143.
[12] A.E. Yılmaz, R. Boncukcuoğlu, M.M. Kocaker¥m, E. Kocadağistan, An empirical model for kinetics of boron removal from boron containing wastewaters by the electrocoagulation method in a batch reactor, Desalination 230 (2008) 288–297.
[13] A.K. Golder, A.K. Chanda, A.N. Samanta, S. Ray, Removal of Cr(VI) from aqueous solution: Electrocoagulation vs chemical coagulation, Sep. Sci. Technol. 42 (2007) 2177–2193.
[14] I. Heidmann, W. Calmano, Removal of Cr(VI) from model wastewater by electrocoagulation with Fe electrodes, Sep. Purif. Technol. 61 (2008) 15–21.
[15] I. Heidmann, W. Calmano, Removal of Zn(II), Cu(II), Ni(II), Ag(II) and Cr(VI) present in aqueous solutions by aluminum electrocoagulation, J. Hazard. Mater. 152 (2008) 934–941.
[16] Z. Zaroual, H. Chaair, A.H. Essadki, K. EI Ass, M. Azzi, Optimizing the removal of trivalent chromium by electrocoagulation using experimental design, Chem. Eng. J. 148 (2009) 488–495.
[17] T. Olmez, The optimization of Cr(VI) reduction and removal by electrocoagulation using response surface methodology, J. Hazard. Mater. 162 (2009) 1371–1378.
[18] M.S. Bhatti, A.S. Reddy, A.K. Thukral, Electrocoagulation removal of Cr(VI) from simulated wastewater using response surface methodology, J. Hazard. Mater. 172 (2009) 839–845.
[19] G. Mouedhen, M. Feki, M.D.P. Wery, H.F. Ayedi, Electrochemical removal of Cr(VI) from aqueous media using iron and aluminum as electrode materials: Towards a better understanding of the involved phenomena, J. Hazard. Mater. 168 (2009) 983–991.
[20] S. Aber, A.R. Amani-Ghadim, V. Mirzajani, Removal of Cr(VI) from polluted solutions by electrocoagulation: Modeling of experimental results using artificial neural network, J. Hazard. Mater. 171 (2009) 484–490.
[21] I. Zongo, J.P. Leclerc, H.A. Maiga, J. Wethe, F. Lapicque, Removal of hexavalent chromium from industrial wastewater by electrocoagulation: A comprehensive comparison of aluminum and iron electrodes, Sep. Purif. Tech. 66 (2009) 159–166.
[22] N.V. Narayana, M. Ganesan, Use of adsorption using granular activated carbon (GAC) for the enhancement of removal of chromium from synthetic wastewater by electrocoagulation, J. Hazard. Mater. 161 (2009) 575–580.
[23] M. Malakootian, H.J. Mansoorian, M. Moosazadeh, Performance evaluation of electrocoagulation process using iron-rod electrodes for removing hardness from drinking water, Desalination 255 (2010) 67–71.
[24] N. Daneshvar, A.R. Khataee, N. Djafarzadeh, The use of artificial neural network (ANN) for modeling of discoloration of textile dye solution containing C.I. basic yellow 28 by electrocoagulation process, J. Hazard. Mater. 137 (2006) 1788–1795.
[25] A. Aleboyeh, N. Daneshvar, M.B. Kasiri, Optimization of C.I. Acid Red 14 dye removal by electrocoagulation batch process with response surface methodology, Chem. Eng. Process. 47 (2008) 827–832.
[26] S. Zodi, O. Potier, F. Lapicque, J.P. Leclerc, Treatment of the industrial wastewaters by electrocoagulation: Optimization of coupled electrochemical and sedimentation processes, Desalination 261 (2010) 186–190.
[27] B.K. Korbahti, Response surface optimization of electrochemical treatment of textile dye wastewater, J. Hazard. Mater. 145 (2007) 277–286.
[28] B.K. Korbahti, A. Tanyolac, Electrochemical treatment of simulated textile wastewater with industrial components and Levafix Blue CA reactive dye: Optimization through response surface methodology, J. Hazard. Mater. 151 (2008) 422–431.
[29] B.K. Korbahti, N. Aktas, A. Tanyolaç, Optimization of electrochemical treatment of industrial paint wastewater with response surface methodology, J. Hazard. Mater. 148 (2007) 83–90.
[30] G. Güven, A. Perendeci, A. Tanyolaç, Electrochemical treatment of deproteinated whey wastewater and optimization of treatment conditions with response surface methodology, J. Hazard. Mater. 157 (2008) 69–78.
[31] M. Tir, N. Moulai-Mostefa, Optimization of oil removal from oily wastewater by electrocoagulation using response surface method, J. Hazard. Mater. 158 (2008) 107–115.
[32] A.W.W.A. APHA, WEF, Standard methods for the examination of water and wastewater, 20th ed.APHA, Washington, DC, 1998.
[33] D.C. Montgomery, Design and Analysis of Experiments, 5th ed.Wiley, New York, 2004.
[34] N.R. Draper, H. Smith, Applied Regression Analysis, 3rd ed., Wiley, New York, 2004.
[35] G.E.P. Box, D.R. Cox, An analysis of transformations, J. R. Stat. Soc., B 26 (1964) 211–243.
[36] Design-Expert Software Version 8.0.0 User's Guide, 2009.
[37] R.H. Myers, D.C. Montgomery, Response Surface Methodology: Process and Product Optimization Using Designed Experiments, Wiley, New York, 1995.